Frequency-entanglement preparation based on the coherent manipulation of frequency nondegenerate energy-time entangled state

Qiang Zhou,[1,3,4] Shuai Dong,[1] Wei Zhang,[1,*] Lixing You,[2] Yuhao He,[2] Weijun Zhang,[2] Yidong Huang,[1] and Jiangde Peng[1]

[1]*Tsinghua National Laboratory for Information Science and Technology, Department of Electronic Engineering, Tsinghua University, Beijing 100084, China*
[2]*State Key Laboratory of Functional Materials for Informatics, Shanghai Institute of Microsystem and Information Technology, Chinese Academy of Sciences, Shanghai 200050, China*
[3]*School of Optoelectronic Information, University of Electronic Science and Technology of China, 610054, China*
[4]*e-mail: betterchou@gmail.com*
**Corresponding author: zwei@tsinghua.edu.cn*

Received April 9, 2014; accepted June 5, 2014;
posted June 6, 2014 (Doc. ID 209653); published July 9, 2014

In this paper, a scheme for frequency-entanglement preparation is proposed and demonstrated based on the coherent manipulation of the frequency nondegenerate energy-time entangled state through an unbalanced Mach–Zehnder interferometer (UMZI). The principle of the coherent manipulation process is analyzed theoretically and demonstrated by experiments of nonclassical two-photon interference under different phase differences between the two arms in the UMZI, showing a fringe visibility of $(96.9 \pm 1.0)\%$. The frequency-entangled two-photon state can be prepared under a proper phase difference, which is demonstrated by an experiment of spatial quantum beating with a fitting visibility of $(99.0 \pm 0.8)\%$. The proposed scheme provides a simple and general way to prepare frequency-entangled states from the frequency nondegenerate energy-time entangled state, which can be easily realized through setups based on fiber optics.

OCIS codes: (270.0270) Quantum optics; (190.4370) Nonlinear optics, fibers; (270.5585) Quantum information and processing.
http://dx.doi.org/10.1364/JOSAB.31.001801

1. INTRODUCTION

Frequency entanglement is a basic quantum resource for applications of scalable quantum networks [1,2], improved quantum communication through noisy quantum channels [3], high-capacity quantum communication and cryptography [4–6], enhanced quantum clock synchronization [7,8], and dispersion nonlocally canceled quantum interferometry [9]. Recently, several schemes for frequency-entangled state preparation have been proposed and demonstrated based on different spontaneous nonlinear parametric processes, such as spontaneous downconversion (SPDC) in nonlinear crystal waveguides [10], spontaneous four-wave mixing (SFWM) in optical fibers [11,12], and silicon waveguides [13]. The principles of these schemes are very similar. First, the spontaneous nonlinear parametric processes generate two coherent frequency nondegenerate correlated states in two optical paths, utilizing the same pump light source and leading to a spatial bunched path-entangled state. Then quantum interference between the two frequency nondegenerate correlated states are realized based on linear optical components such as a 50/50 beam splitter, 50/50 fiber coupler, or polarization beam splitter, transforming the spatial bunched path-entangled state to a spatial antibunched path-entangled state, which is exactly the frequency-entangled state due to the frequency nondegenerate property. The quantum interference process can be viewed as coherent manipulation between the two kinds of the spatial path-entangled states. Since the coherent manipulation is a general way to transform the quantum states coherently, it can be expected that many different kinds of entangled states could be utilized to prepare frequency entanglement, if proper coherent manipulation designs are found.

On the other hand, the frequency nondegenerate energy-time entangled state is one of the most commonly used entangled states in experiments of quantum optics, which can be easily generated by SPDC in second-order nonlinear optical components [10], and SFWM in third-order nonlinear optical waveguides [11–13]. In this paper, we propose and demonstrate a scheme of frequency-entanglement preparation based on the coherent manipulation of the frequency nondegenerate energy-time entangled state utilizing unbalanced Mach–Zehnder interferometers (UMZI). Thanks to the time delay between the two arms in the UMZI, the wavefunction of the injected energy-time entangled state is divided into two parts at the first 50/50 coupler and interfere with each other at the second 50/50 coupler, if the coherence time of the wavefunction is greater than the time delay between the two arms. A superposition of the spatial bunched and antibunched path-entangled states would be obtained at the

output ports of UMZI by applying a time domain filter on the coincidence measurement. The superposition coefficients of the two path-entangled states are controlled by the phase difference between the two arms in the UMZI. A pure spatial antibunched path-entangled state can be prepared under a certain phase difference, which is the two-photon state with frequency-entanglement property. In the experiment, the principle of coherent manipulation process is demonstrated by nonclassical two-photon interference (TPI) under different phase difference, with a visibility of $(96.9 \pm 1.0)\%$. The frequency-entanglement property of the frequency-entangled state is verified by a spatial quantum beating experiment with a visibility of $(99.0 \pm 0.8)\%$. The experiment results show that the proposed scheme provides a simple and general way to prepare frequency entanglement based on the generation of a frequency nondegenerate energy-time entangled state, which can be easily realized through setups based on fiber optics.

This paper is organized as follows. First, the principle of the coherent manipulation of a frequency nondegenerate energy-time entangled state in an UMZI is introduced in Section 2. The experiment demonstration of coherent manipulation is shown in Section 3, which is based on a commercial UMZI and frequency nondegenerate energy-time entangled state generated in optical fibers. Then the preparation of a frequency entangled state and its spatial quantum beating experiment is presented in Section 4. We close the paper with a summary.

2. PRINCIPLE OF COHERENT MANIPULATION IN UMZI

Figure 1(a) shows the structure of an UMZI, which consists of two 50/50 couplers, an optical delay line with a delay time of τ, and a phase modulator introducing a relative phase difference of φ between the two arms. The UMZI is a four-port linear optical device with two input spatial modes, a and b, and two output spatial modes, c and d. Let the frequency nondegenerate correlated state of $|\omega_i\omega_s\rangle_a$ with energy-time entanglement property be injected into the UMZI from port a, where ω_i and ω_s are the angular frequencies of idler and signal photons, respectively. For simplicity, the behaviors of the two 50/50 couplers, optical delay line, and phase modulator in the UMZI are all assumed to be frequency independent. In this case, the output two-photon state of the first 50/50 coupler is

$$\begin{aligned}|\zeta_0\rangle &= \frac{1}{\sqrt{2}}(|\psi_1'\rangle + i|\psi_2'\rangle),\\ |\psi_1'\rangle &= \frac{1}{\sqrt{2}}(|\omega_i\rangle_S|\omega_s\rangle_S - |\omega_i\rangle_L|\omega_s\rangle_L),\\ |\psi_2'\rangle &= \frac{1}{\sqrt{2}}(|\omega_i\rangle_S|\omega_s\rangle_L + |\omega_s\rangle_L|\omega_i\rangle_S),\end{aligned} \tag{1}$$

where $|\omega_{i,s}\rangle_S$ and $|\omega_{i,s}\rangle_L$ are the states of the idler or signal photon, which propagate along the short and long arms of the UMZI, respectively. Hence, $|\psi_1'\rangle$ is the spatial bunched path-entangled state, i.e., two photons are in the same path simultaneously; $|\psi_2'\rangle$ is the spatial antibunched path-entangled state, i.e., two photons are in different paths simultaneously.

The output two-photon state of the first 50/50 coupler naturally evolves along the two arms and meets at the second 50/50 coupler. For two photons in the state of $|\psi_1'\rangle$, they travel along the same arm and output from the UMZI simultaneously; for two photons in the state of $|\psi_2'\rangle$, they travel along two arms separately and output from the UMZI with time delays of $\Delta t = t_s - t_i = \pm\tau$, where t_s and t_i are the output moments of signal and idler photons, respectively. The contributions of $|\psi_1'\rangle$ and $|\psi_2'\rangle$ in the output two-photon states are distinguished by the time-resolved two-photon coincidence measurement. If a time domain filter is applied to select two-photon states with $\Delta t = 0$ and reject the ones with $\Delta t = \pm\tau$, the contribution of $|\psi_1'\rangle$ can be selected as shown in Fig. 1(b). It is found that half of the two-photon pairs in the input two-photon states is selected, while the other half is lost. If the single-photon coherence time of the signal or idler photon is much smaller than the delay time τ in the UMZI, the single-photon interference is prevented, where the single-photon coherence time is denoted by τ_{coh}, which is determined by the spectral width of the generated signal or idler photon. For the frequency nondegenerate energy-time entangled state generated in optical fibers, the generated signal and idler photons have wide spectral widths, satisfying the condition $\tau_{\mathrm{coh}} \ll \tau$ [14,15]. Under this condition, the two-photon states selected by the time domain filter can be derived as

$$\begin{aligned}|\zeta_1\rangle &= \frac{1}{\sqrt{2}}\begin{pmatrix}(1 + e^{i((\omega_s+\omega_i)\tau+2\varphi)})|\psi_1\rangle +\\ i(1 - e^{i((\omega_s+\omega_i)\tau+2\varphi)})|\psi_2\rangle\end{pmatrix},\\ |\psi_1\rangle &= \frac{1}{\sqrt{2}}(|\omega_i\rangle_c|\omega_s\rangle_c - |\omega_i\rangle_d|\omega_s\rangle_d),\\ |\psi_2\rangle &= \frac{1}{\sqrt{2}}(|\omega_i\rangle_c|\omega_s\rangle_d + |\omega_i\rangle_d|\omega_s\rangle_c),\end{aligned} \tag{2}$$

where $|\omega_{i,s}\rangle_c$ and $|\omega_{i,s}\rangle_d$ are states of the output idler or signal photons at port c and d, respectively; $|\psi_1\rangle$ and $|\psi_2\rangle$ are spatial bunched and antibunched path-entangled states at the output of the UMZI, respectively; and $(\omega_i + \omega_s)\tau$ is a constant determined by the frequency ω_p of pump light, i.e., $\omega_i + \omega_s = 2\omega_p$, and the delay time τ in the UMZI. The derivation of Eq. (2) requires that the coherence time T_c of the $|\psi_1'\rangle$ is far larger than τ, i.e., $T_c \gg \tau$. However, T_c is limited in experiment, which influences the quantum interference as illustrated in Fig. 1(c). When $T_c \le \tau$, the two-photon wave function of $|\psi_1'\rangle$ does not interfere with itself, since the wave functions through the two arms of the UMZI are separated in time; while $T_c > \tau$, wave function of $|\psi_1'\rangle$ partially interferes with itself because the wave functions through the UMZI are overlapped in the

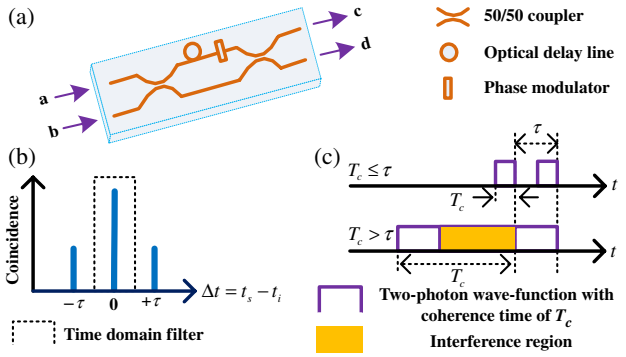

Fig. 1. Scheme for the coherent manipulation of a frequency nondegenerate energy-time entangled state in an UMZI. (a) Structure of an UMZI. (b) Time-resolved two-photon coincidence measurement. (c) Interference property of selected two-photon states.

time region from τ to T_c. Equation (2) shows that the two-photon state output from the UMZI is a superposition state of spatial bunched and antibunched path-entangled states. The output possibilities of the two two-photon states are controlled by φ, which are expressed as

$$P_1 = 0.5 \times (1 + \cos((\omega_s + \omega_i)\tau + 2\varphi)),$$
$$P_2 = 0.5 \times (1 - \cos((\omega_s + \omega_i)\tau + 2\varphi)), \quad (3)$$

where P_1 and P_2 are the output possibilities of $|\psi_1\rangle$ and $|\psi_2\rangle$, respectively. It can be seen that P_1 and P_2 periodically vary with φ, while the sum of them equals to 1 under any φ. Similar results also can be obtained while other energy-time entangled states are input into the UMZI such as $|\omega_i\omega_s\rangle_b$, $|\omega_i\rangle_b|\omega_s\rangle_a$, and $|\omega_i\rangle_a|\omega_s\rangle_b$.

3. EXPERIMENTAL DEMONSTRATION OF COHERENT MANIPULATION IN UMZI

The theoretical analysis shows that if the coherence time T_c of the two-photon state is larger than the delay time τ in the UMZI, the energy-time entangled state is coherently manipulated in an UMZI. A superposition state of spatial bunched and antibunched path-entangled states can be selected by a time domain filter, as shown in Eq. (2). The superposition coefficients or output possibilities of the two path-entangled states are controlled by the phase difference φ in the UMZI.

Figure 2 shows the setup for the experimental demonstration. Figure 2(a) is the setup for a frequency nondegenerate energy-time entangled state generation in optical fiber. A piece of dispersion-shifted fiber (DSF, 800 meters in length, Yangtze Co. Ltd.) is pumped by a continuous wave (CW) monochromatic laser (Agilent 81980A) with a linewidth of 100 kHz. The wavelength of pump light is set as 1552.16 nm, closing to the zero dispersion wavelength $\lambda_0 = 1549$ nm of the DSF. To reduce the Raman noise photons generated from spontaneous Raman scattering, the DSF is cooled in liquid nitrogen [16,17]. The power of pump light is amplified by an erbium-doped fiber amplifier (EDFA). A variable optical attenuator (VOA) and a 99/1 fiber coupler with a power meter (PM) is used to control and monitor the pump power level, which is 10 mW in the experiment. The sideband noise photons in the pump light are rejected by a pump filter with a sideband rejection of greater than 120 dB [18]. The energy-time entangled state is generated by the SFWM process in DSF, and the generated entangled states are wavelength nondegenerate. The coherence time T_c of the obtained entangled state is about 10 μs (equaling to the coherence time of pump light estimated by its linewidth), implying that the emission moment of a two-photon pair is unpredictable in a 10 μs time domain window.

The generated energy-time entangled state is directly injected into the UMZI from port a, as shown in Fig. 2(b). The UMZI used in the experiment is a part of a commercial 10 GHz differential quaternary phase-shift keying (DQPSK) demodulator for coherent optical fiber communication (Optoplex Corp., DI-CAKFASO15-R1). The total insertion loss of the device is 4.2 dB, including an additional loss of 3 dB introduced by the addition of a 50/50 splitter. The time delay of τ between the two arms is 100 ps. At the output end of the UMZI, the two-photon state outputs from ports B and C, corresponding to ports c and d of the UMZI shown in Fig. 1(a), respectively. Signal and idler photons satisfying the energy conservation are selected by two filtering and splitting modules with insertion losses of 0.8 dB, (F&S Modules 1 and 2) as shown in Fig. 2(c). The selected wavelengths of signal and idler photons

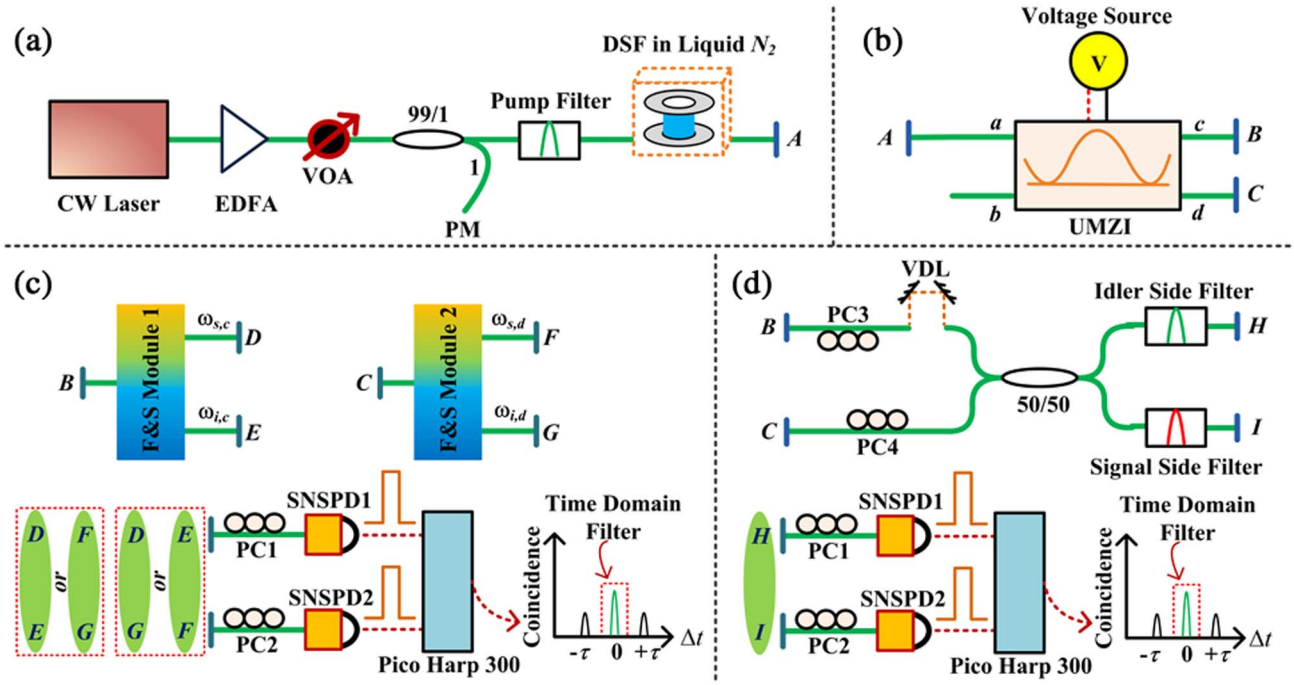

Fig. 2. Experiment setups. (a) Setup for the generation of frequency nondegenerate energy-time entangled state: EDFA, erbium-doped fiber amplifier; VOA, variable optical attenuator; PM, power meter; DSF, dispersion shifted fiber; 99/1, 99/1 coupler. (b) Structure of the UMZI used in the experiment. (c) Setups for nonclassical TPI: F&S, filtering and splitting system; SNSPD, superconducting nanowire single photon detector; PC, polarization controller. (d) Setups for measuring spatial quantum beating: VDL, variable delay line; 50/50, 50/50 coupler.

are centered at 1555.75 and 1549.32 nm, respectively, with a −3 dB spectral width of $2\pi \times 32$ GHz. A pump light isolation of greater than 120 dB is achieved in the two F&S modules [18]. The coherent time τ_{coh} of the filtered signal and idler photons is about 30 ps, which is estimated by the spectral widths of the filters. Hence, single-photon interference is eliminated in the UMZI due to $\tau_{\mathrm{coh}} < \tau$. On the other hand, τ is much smaller than the T_{c} of 10 μs, which ensures that the two-photon state can interfere with itself in the UMZI. The photon state output from ports D, E, F, and G correspond to the $|\omega_s\rangle_c$, $|\omega_i\rangle_c$, $|\omega_s\rangle_d$, and $|\omega_i\rangle_d$ states in Eq. (2), respectively. The phase difference φ is controlled by the applied voltage of the UMZI shown in Fig. 2(b).

The spatial bunched and antibunched path-entangled states can be distinguished by coincidence measurement with different combinations of the output ports, which are measured by a time-resolved two-photon coincidence measurement in the experiment. To measure the spatial bunched path-entangled states, ports D and E (or F and G) are connected to two superconducting nanowire single-photon detectors (SNSPD 1 and 2), respectively; while for spatial antibunched path-entangled states, ports D and G (or E and F) are connected to SNSPD 1 and 2, respectively. Two polarization controllers (PC1 and PC2) are placed before SNSPDs to adjust the polarization state of photons, since the detection efficiencies of the SNSPDs are polarization dependent. The SNSPD 1 and 2 are installed in one Gifford–McMahon cryocooler at a working temperature of 2.2 K, with a detection efficiency of 6.0% and 4.0% under a dark count rate of 10 Hz, respectively; the timing jitters of SNSPD 1 and 2 are 25 and 44 ps, respectively [19]. The output of SNSPDs are sent into a time-correlated single-photon counting module (TCSPC, PicoHarp 300, PicoQuant) for time-resolved two-photon coincidence measurement, in which the used time-bin width is 4 ps. Thanks to the small timing jitters of SNSPDs and the high time resolution of the TCSPC module, a high-resolution time-resolved two-photon coincidence measurement is obtained, and a very narrow time domain filter is applied to select two-photon states in the experiment.

Figure 3 shows a typical result of the time-resolved two-photon coincidence measurement. The spatial antibunched path-entangled states are measured with ports E and F connected to SNSPDs. The bars and squares are experimental results under φ of $\pi/2$ and π, while solid and dashed lines are the Gaussian fitting envelopes for eye guiding. Three distinct coincidence peaks are obtained with a 100 ps time delay between adjacent peaks, which corresponds to the τ in the UMZI. Every single peak has a fitting full width at half-maximum (FWHM) width of 35 ps, which is mainly caused by the timing jitters of SNSPDs. The central peak corresponds to the coincidence count of antibunched path-entangled states, which are obtained with high fidelity by applying a time domain filter of 88 ps, as shown in Fig. 3. The accidental coincidence counts caused by noise counts are measured by shifting the time domain filter out of the three coincident peaks and calculating the sum of the background coincidence counts in it. It can be calculated that the coincidence to accidental coincidence ratio (CAR) is 32 ± 5 in the experiment. The central coincidence peak vanishes when $\varphi = \pi$, which indicates that no spatial antibunched path-entangled state exits from the UMZI as predicted by Eqs. (2) and (3).

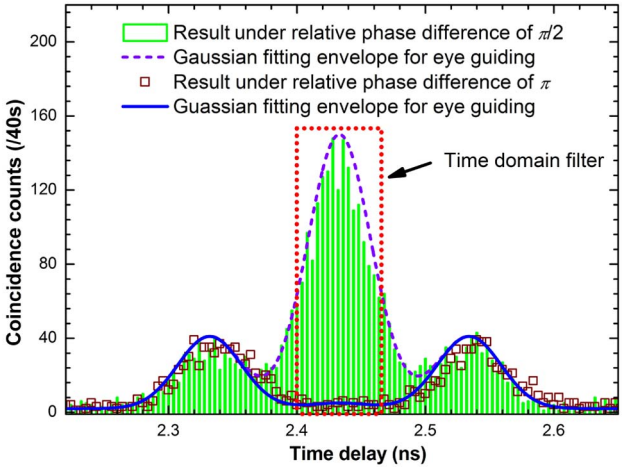

Fig. 3. Typical time-resolved two-photon coincidence measurement results. The bars and squares are experiment results under φ and equal to $\pi/2$ and π, respectively; dashed and solid lines are Gaussian fitting envelopes for eye guiding.

The coherent manipulation of the frequency nondegenerate energy-time entangled state generated in optical fibers is measured through a nonclassical TPI experiment. In the experiment, the coincidence counts of the spatial bunched and antibunched path-entangled states are measured under different φ, as shown in Fig. 4, in which coincidence counts are the sum over the central coincidence peak in a time domain filter of 88 ps. Figure 4(a) shows the measured results of the spatial antibunched path-entangled states measured by connecting ports E and F to SNSPD 1 and 2, respectively. Circles are experiment results, while the solid line is the fitting curve of the nonclassical TPI interference, according to Eq. (3), showing a fitting visibility of $(96.9 \pm 1.0)\%$, without subtracting the accidental coincidence counts. Figure 4(b) shows the measured results of the spatial bunched path-entangled states measured by connecting ports D and E to SNSPD 1 and 2, respectively. Squares are experiment results, while the solid line is the fitting curve, also showing a fitting visibility of $(96.9 \pm 1.0)\%$, without subtracting the accidental coincidence counts. It is shown that the coincidence counts in the two spatial path-entangled states vary with φ under a period of π, while the single-photon counts of signal and idler sides do not vary with φ, as shown in the insets of Fig. 4. The results indicate that the coherent manipulation of the frequency nondegenerate energy-time entangled state generated in an optical fiber is observed in our experiment. The output two-photon state of the UMZI is a superposition state of the spatial bunched and antibunched path-entangled states, which is controlled by φ. Pure spatial antibunched or bunched path-entangled t states can be prepared by setting φ as $(k + 0.5)\pi$ or $k\pi$ (k is an integer), respectively. The pure antibunched path-entangled state is exactly the prepared frequency entangled state.

4. SPATIAL QUANTUM BEATING EXPERIMENT OF FREQUENCY ENTANGLED STATE

In the experiment, we obtain the frequency-entangled state under $\varphi = 1.5\pi$. The frequency-entanglement property is demonstrated by the spatial quantum beating. Figure 2(d) shows the experiment setups. The two-photon state from ports B and C is input into a 50/50 fiber coupler with a relative arrival time

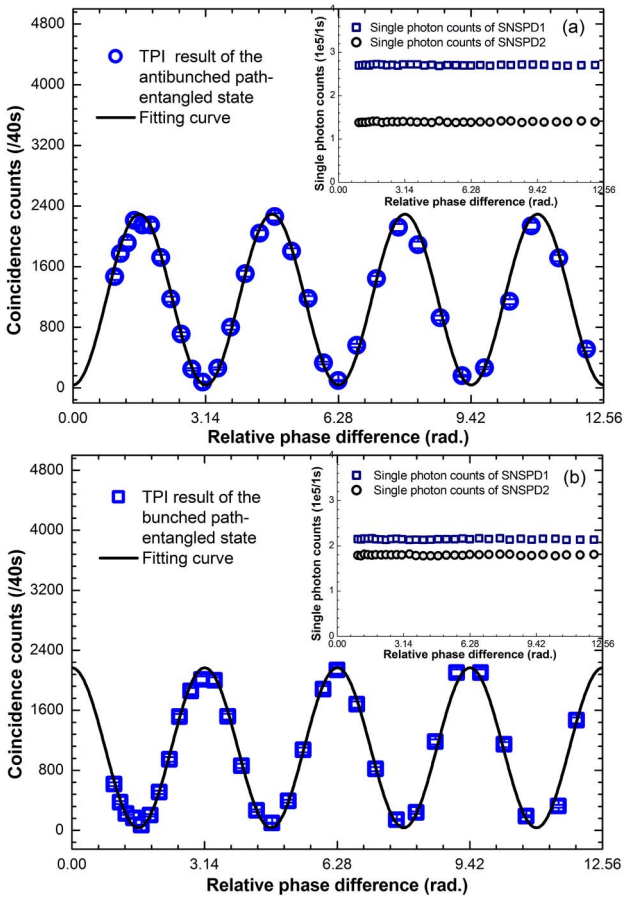

Fig. 4. Nonclassical TPI of spatial bunched and antibunched path-entangled states measured under different φ. (a) Results of spatial antibunched path-entangled states: circles are experiment results; solid line is fitting curve with a visibility of $(96.9 \pm 1.0)\%$. (b) Result of spatial bunched path-entangled states: squares are experiment results; solid line is fitting curve with a visibility of $(96.9 \pm 1.0)\%$; inserts of (a) and (b) are single-side photon count rates.

delay of $\Delta\tau$ between the two photons, which is controlled by a variable delay line (VDL, MDL-002, General Photonics Corp.). PC 3 and 4 are used to ensure that the input photons of a 50/50 coupler are in an identical polarization state. At the output ports of the 50/50 coupler, photons pass through signal and idler side filters and are detected by SNSPD 1 and 2, respectively. The outputs of two SNSPDs are sent into time-resolved two-photon coincidence measurement system to obtain coincidence counts. Normalized coincidence counts can be expressed as [20]

$$P_{co} \propto 1 - V_0\xi(\sigma \times \Delta\tau)\cos(|v_i - v_s| \times \Delta\tau) \times \xi(\sigma \times \Delta\tau) = \mathrm{sinc}(\sigma \times \Delta\tau), \quad (4)$$

where V_0 is the visibility of spatial beating TPI; $\xi(\sigma \times \Delta\tau)$ is a function related to spectral properties of signal and idler photons, which is $\mathrm{sinc}(\sigma \times \Delta\tau)$ due to the signal and idler side filters being Gaussian shaped, with an angular frequency bandwidth of $\sigma = 2\pi \times 32 \times 10^9$ in the experiment; and $v_{i,s}$ is the frequency of idler and signal photons, the frequency spacing of them is 800 GHz in the experiment. Figure 5 shows the result of the spatial quantum beating. The coincidence counts also are obtained by summing the central coincidence

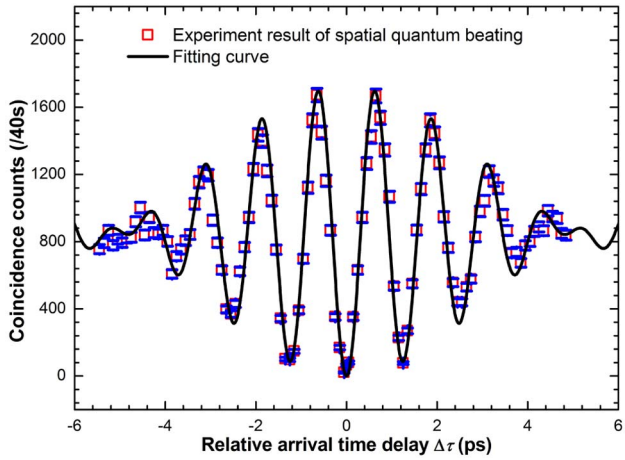

Fig. 5. Spatial quantum beating of frequency entangled state; squares are experiment results; solid line is the fitting curve with a fitting visibility of $(99.0 \pm 0.8)\%$.

peak in a time domain filter of 88 ps. Squares are experiment results. The solid line is a fitting curve according to Eq. (4), showing a visibility of $(99.0 \pm 0.8)\%$, without subtracting the accidental coincidence counts. The period of spatial quantum beating fringe is 1.25 ps, i.e., a period of 375 μm in length, which is determined by the frequency spacing between the idler and signal photons. It can be seen that the experiment result agrees well with Eq. (4), demonstrating the frequency-entanglement property of the obtained two-photon state. The fidelity of the obtained frequency-entangled state is $(99.5 \pm 0.4)\%$, calculated by $F = (1 + V_0)/2$ [11].

5. SUMMARY

In summary, we proposed and experimentally demonstrated a simple and general scheme of frequency-entanglement preparation based on the coherent manipulation of the frequency nondegenerate energy-time entangled state utilizing an UMZI. A superposition of the spatial bunched and antibunched path-entangled states is obtained through the coherent manipulation process, which is selected by a time domain filter at the output of the UMZI. The superposition coefficients or output possibilities of the two states are controlled by the phase difference between the two arms in the UMZI. A pure frequency-entangled state, i.e., spatial antibunched path-entangled state, can be prepared under a phase difference of 1.5π. Experiments of nonclassical TPI are realized to demonstrate the proposed coherent manipulation scheme, showing a fringe visibility of $(96.9 \pm 1.0)\%$. A pure frequency-entangled state is prepared in the experiment, which is demonstrated by an experiment of spatial quantum beating with a fitting visibility of $(99.0 \pm 0.8)\%$. It is worth noting that, although the scheme is demonstrated by setups based on fiber optics, as a general scheme, it can be applied on the frequency nondegenerate energy-time entangled state generated by any mechanism, such as SFWM in silicon waveguides and chalcogenide As_2S_3 waveguides [13,21–23], which are desired in integrated quantum photonics.

ACKNOWLEDGMENTS

This work is supported by the 973 Programs of China under contract nos. 2010CB327606 and 2011CBA00303, the China

Postdoctoral Science Foundation, the National Natural Science Foundation of China under contract no. 91121022 and 61321004, and the Strategic Priority Research Program (B) of the Chinese Academy of Sciences under contract nos. XDB04010200 and XDB04020100; research startup funds of the University of Electronic Science and Technology of China (UESTC) under contract no. Y02002010501062 and the project sponsored by the Oversea Academic Training Funds, OATF of UESTC.

REFERENCES

1. H. J. Kimble, "The quantum internet," Nature **453**, 1023–1030 (2008).
2. L. M. Duan and C. Monroe, "Colloquium: quantum networks with trapped ions," Rev. Mod. Phys. **82**, 1209–1224 (2010).
3. L. Xiao, C. Wang, W. Zhang, Y. Huang, J. Peng, and G. Long, "Efficient strategy for sharing entanglement via noisy channels with doubly entangled photon pairs," Phys. Rev. A **77**, 042315 (2008).
4. M. Fujiwara, M. Takeoka, J. Mizuno, and M. Sasaki, "Exceeding the classical capacity limit in a quantum optical channel," Phys. Rev. Lett. **90**, 167906 (2003).
5. D. Bruss and C. Macchiavello, "Optimal eavesdropping in cryptography with three-dimensional quantum states," Phys. Rev. Lett. **88**, 127901 (2002).
6. N. J. Cerf, M. Bourennane, A. Karlsson, and N. Gisin, "Security of quantum key distribution using *d*-level systems," Phys. Rev. Lett. **88**, 127902 (2002).
7. M. de Burgh and S. D. Bartlett, "Quantum methods for clock synchronization: beating the standard quantum limit without entanglement," Phys. Rev. A **72**, 042301 (2005).
8. V. Giovannetti, S. Lloyd, and L. Maccone, "Quantum-enhanced positioning and clock synchronization," Nature **412**, 417–419 (2001).
9. O. Minaeva, C. Bonato, B. E. A. Saleh, D. S. Simon, and A. V. Sergienko, "Odd- and even-order dispersion cancellation in quantum interferometry," Phys. Rev. Lett. **102**, 100504 (2009).
10. S. Ramelow, L. Ratschbacher, A. Fedrizzi, N. K. Langford, and A. Zeilinger, "Discrete tunable color entanglement," Phys. Rev. Lett. **103**, 253601 (2009).
11. X. Li, L. Yang, X. Ma, L. Cui, Z. Y. Ou, and D. Yu, "All-fiber source of frequency-entangled photon pairs," Phys. Rev. A **79**, 033817 (2009).
12. Q. Zhou, W. Zhang, C. Yuan, Y. Huang, and J. Peng, "Generation of 1.5 μm discrete frequency-entangled two-photon state in polarization-maintaining fibers," Opt. Lett. **39**, 2109–2112 (2014).
13. J. W. Silverstone, D. Bonneau, K. Ohira, N. Suzuki, H. Yoshida, N. Iizuka, M. Ezaki, C. M. Natarajan, M. G. Tanner, R. H. Hadfield, V. Zwiller, G. D. Marshall, J. G. Rarity, J. L. O'Brien, and M. G. Thompson, "On-chip quantum interference between silicon photon-pair sources," Nat. Photonics **8**, 104–108 (2014).
14. E. Brainis, "Four-photon scattering in birefringent fibers," Phys. Rev. A **79**, 023840 (2009).
15. Q. Zhou, W. Zhang, J. Cheng, Y. Huang, and J. Peng, "Noise performance comparison of 1.5 μm correlated photon pair generation in different fibers," Opt. Express **18**, 17114–17123 (2010).
16. H. Takesue and K. Inoue, "Generation of 1.5-μm band time-bin entanglement using spontaneous fiber four-wave mixing and planar light-wave circuit interferometers," Phys. Rev. A **72**, 041804(R) (2005).
17. Q. Zhou, W. Zhang, P. Wang, Y. Huang, and J. Peng, "Polarization entanglement generation at 1.5 μm based on walk-off effect due to fiber birefringence," Opt. Lett. **37**, 1679–1681 (2012).
18. Q. Zhou, W. Zhang, T. Niu, S. Dong, Y. Huang, and J. Peng, "A polarization maintaining scheme for 1.5 μm polarization entangled photon pair generation in optical fibers," Eur. Phys. J. D **67**, 202 (2013).
19. L. You, X. Yang, Y. He, W. Zhang, D. Liu, W. Zhang, L. Zhang, L. Zhang, X. Liu, S. Chen, Z. Wang, and X. Xie, "Jitter analysis of a superconducting nanowire single photon detector," AIP Advances **3**, 072135 (2013).
20. Z. Y. Ou and L. Mandel, "Observation of spatial quantum beating with separated photodetectors," Phys. Rev. Lett. **61**, 54–57 (1988).
21. N. Lv, W. Zhang, Y. Guo, Q. Zhou, Y. Huang, and J. Peng, "1.5 μm polarization entanglement generation based on birefringence in silicon wire waveguides," Opt. Lett. **38**, 2873–2876 (2013).
22. N. Matsuda, H. Takesue, K. Shimizu, Y. Tokura, E. Kuramochi, and M. Notomi, "Slow light enhanced correlated photon pair generation in photonic-crystal coupled-resonator optical waveguides," Opt. Express **21**, 8596–8604 (2013).
23. C. Xiong, G. Marshall, A. Peruzzo, M. Lobino, A. Clark, D. Choi, S. Madden, C. Natarajan, M. Tanner, R. Hadfield, S. Dorenbos, T. Zijlstra, V. Zwiller, M. Thompson, J. Rarity, M. Steel, B. Luther-Davies, B. Eggleton, and J. O'Brien, "Generation of correlated photon pairs in a chalcogenide As_2S_3 waveguide," Appl. Phys. Lett. **98**, 051101 (2011).